



GABAergic parafacial zone is a medullary slow-wave-sleep promoting center

Citation

Anacleto, Christelle, Loris Ferrari, Elda Arrigoni, Caroline E. Bass, Clifford B. Saper, Jun Lu, and Patrick M. Fuller. 2014. "GABAergic parafacial zone is a medullary slow-wave-sleep promoting center." *Nature neuroscience* 17 (9): 1217-1224. doi:10.1038/nn.3789. <http://dx.doi.org/10.1038/nn.3789>.

Published Version

doi:10.1038/nn.3789

Permanent link

<http://nrs.harvard.edu/urn-3:HUL.InstRepos:14351306>

Terms of Use

This article was downloaded from Harvard University's DASH repository, and is made available under the terms and conditions applicable to Other Posted Material, as set forth at <http://nrs.harvard.edu/urn-3:HUL.InstRepos:dash.current.terms-of-use#LAA>

Share Your Story

The Harvard community has made this article openly available.
Please share how this access benefits you. [Submit a story](#).

[Accessibility](#)

Published in final edited form as:

Nat Neurosci. 2014 September ; 17(9): 1217–1224. doi:10.1038/nn.3789.

GABAergic parafacial zone is a medullary slow-wave-sleep promoting center

Christelle Anaclet¹, Loris Ferrari¹, Elda Arrigoni¹, Caroline E. Bass², Clifford B. Saper¹, Jun Lu^{1,*}, and Patrick M. Fuller^{1,*}

¹Department of Neurology, Division of Sleep Medicine, Harvard Medical School and Beth Israel Deaconess Medical Center, Boston, MA 02215

²Department of Pharmacology and Toxicology, School of Medicine and Biomedical Sciences, University at Buffalo, Buffalo, NY

Abstract

Work in animals and humans suggest the existence of a slow-wave sleep (SWS) promoting/EEG synchronizing center in the mammalian lower brainstem. While sleep-active GABAergic neurons in the medullary parafacial zone (PZ) are needed for normal SWS, it remains unclear if these neurons can initiate and maintain SWS or EEG slow wave activity (SWA) in behaving mice. We used genetically targeted activation and optogenetic-based mapping to uncover the downstream circuitry engaged by SWS-promoting PZ neurons, and we show that this circuit uniquely and potently initiates SWS and EEG SWA, regardless of the time of day. PZ neurons monosynaptically innervate and release synaptic GABA onto parabrachial neurons that in turn project to and release synaptic glutamate onto cortically-projecting neurons of the magnocellular basal forebrain; hence a circuit substrate is in place through which GABAergic PZ neurons can potently trigger SWS and modulate the cortical EEG.

A “good night’s sleep” is an established prerequisite for optimal physiologic, psychologic and cognitive function, yet the sub-cortical brain structures regulating sleep, in particular slow-wave-sleep (SWS), and its electroencephalogram (EEG) correlates remain incompletely understood. One model of sleep-wake regulation posits a flip-flop switching mechanism that involves mutually inhibitory interactions between sleep-promoting neurons in the ventrolateral preoptic area (VLPO) and wake-promoting neurons in the brainstem and hypothalamus^{1,2}. While this model has heuristic value for understanding the neurobiology of sleep and its disorders, it does not fully account for data derived from early neurophysiologic and transection experiments in animals³⁻⁵ and more recent human-based functional magnetic resonance imaging (fMRI) studies⁶ that have suggested the existence of a SWS-promoting/EEG synchronizing “center” in the lower brainstem of mammals. Even though animals with lesions of the VLPO show a dramatic (ca. 40–50%) and sustained increase in waking, about half of the normal behavioral and electrographic SWS remains⁷, indicating additional circuitry for promoting SWS must exist. The intensity of cortical slow-

Correspondence to: Jun Lu; Patrick M. Fuller.

*Corresponding Authors

wave-activity (SWA: 0.5–4Hz) during SWS is also widely accepted as a reliable indicator of sleep need; is thought to mediate the general restorative function of sleep^{8, 9}; and is thought to play a role in memory consolidation¹⁰, synaptic homeostasis¹¹ and other aspects of cortical plasticity¹². Hence, elucidating the location and identity of extra-VLPO neurons that generate SWS and cortical SWA remains central to our understanding of not only brain sleep *per se* but also many sleep-dependent neurobiological processes. Towards this end, it was recently reported that sleep-active GABAergic neurons in the medullary parafacial zone (PZ) are needed for normal SWS¹³. However it remains unclear if these neurons are capable of driving SWS or EEG SWA in intact animals, and how these putative SWS-promoting PZ neurons may be functionally, synaptically coupled with more rostrally situated circuitry capable of influencing the cortical EEG.

Results

PZ GABAergic neurons promote SWS in behaving mice

To test the ability of GABAergic PZ neurons to initiate SWS in behaving animals, we placed bilateral injections of an adeno-associated viral (AAV) vector containing an excitatory modified muscarinic G protein-coupled receptor (DIO-hM3Dq-mCherry-AAV10; Fig. 1b) expressed in a cre-dependent manner into the PZ (Fig. 1a–b,f–g and Supplementary Fig. 1) of *Vgat-IRE5-cre* mice¹⁴ (Fig. 1c–e) and non-cre expressing littermates. Robust cell-surface expression of the hM3Dq receptors was observed on GABAergic PZ neurons of *Vgat-IRE5-cre* mice (Fig. 1f–g) but was absent in non-cre-expressing littermates, confirming the requirement for cre activity to enable hM3Dq expression within PZ GABAergic neurons. Injections of the hM3Dq agonist clozapine-N-oxide [CNO 0.3mg/kg, intraperitoneal (IP)], which is otherwise pharmacologically inert, also drove c-Fos expression in hM3Dq-expressing GABAergic neurons in the PZ (Fig. 1h), confirming ligand-induced activation of hM3Dq-expressing GABAergic PZ neurons *in vivo*. CNO-driven depolarization and firing of hM3Dq-expressing GABAergic PZ neurons was also confirmed in whole cell, current clamp recordings (Fig. 1i). Importantly, in baseline condition, we observed no differences between *Vgat-IRE5-cre* mice expressing hM3Dq in GABAergic PZ neurons and non-hM3Dq-expressing littermate mice in hourly sleep-wake or the EEG power spectra (Supplementary Fig. 2 and Supplementary Table 1), demonstrating that, in the absence of the ligand (CNO), hM3Dq receptors are without effect on sleep-wake parameters. Similarly, IP injections of CNO were without significant effect on these same parameters in non-hM3Dq-expressing mice (Supplementary Fig. 3 and Supplementary Table 2), indicating that electrographic or physiologic changes observed in hM3Dq-expressing mice following CNO administration is directly linked to the activation of PZ GABAergic neurons.

Following IP vehicle injections at 7PM [lights-off], mice expressing the hM3Dq receptor in GABAergic PZ neurons displayed a typical night hypnogram with long bouts of wakefulness marked by high EMG activity and low EEG SWA (Fig. 2a). Following IP CNO injections however mice fell asleep with a short latency (Fig. 3b and Supplementary Table 2) and SWS, marked by low electromyogram (EMG) activity and high EEG SWA (Fig. 2b–c), was significantly increased during the 3 hr post-injection period as compared with

vehicle (Fig. 3b and Supplementary Table 2). SWS bout length was also significantly increased during the 3 hr post-CNO injection period (Supplementary Table 2), indicating a consolidate CNO-induced SWS. More specifically, when SWS bout duration was analyzed as a function of bout length for baseline or vehicle injection conditions, the preponderance of SWS occurred in 1–10 min bouts, with no bouts exceeding 20 min. (Fig. 3e). Following administration of CNO however the preponderance of SWS occurred in bouts longer than 5 min and ca. 35% of the SWS amount occurred in bouts longer than 20 min. The SWS EEG was also enriched with SWA during the first hour of CNO-induced SWS as compared with SWS following vehicle injection (Fig. 2b, Fig. 3c and Supplementary Fig. 4). By contrast, higher frequencies such as beta and gamma were decreased. Because SWA is a widely accepted marker of SWS quality and intensity^{9, 15, 16} and high EEG frequencies are indicative of cortical activation and wakefulness¹⁷, our findings suggest that GABAergic PZ neurons can influence both the quantitative and qualitative aspects of SWS. SWS delta power is typically maximal during the dark period, following long, consolidated bouts of wakefulness. Interestingly, activation of PZ GABAergic neurons by CNO resulted in higher SWS delta power than the maximum observed during time-of-day equivalent spontaneous sleep in these mice. The same was true when CNO injections were performed during the light period (Fig. 4c), which is a time of high “sleep drive” in mice. Even more significantly, activation of PZ GABAergic neurons by CNO during the normal sleeping period increased SWS amount and bout lengths beyond the maximum observed during time-of-day equivalent spontaneous sleep (Fig. 4b,e and Supplementary Table 2). The consolidated SWS and elevated SWA observed after activation of PZ GABAergic neurons is similar to the sleep rebound following sleep deprivation. Furthermore, the deep SWS induced by CNO administration appeared to satisfy the homeostatic need for sleep for the remainder of the dark period (Fig. 2b). In general agreement with the behavioral and EEG findings, CNO administration produced a marked reduction in cortical c-Fos (Supplementary Fig. 5), indicative of a quiescent cellular cortex. Finally, acute and selective silencing of PZ GABAergic neurons at 10AM (a time of high sleep pressure in the mouse), which we achieved using a cre-enabled inhibitory modified muscarinic G protein-coupled receptor (DIO-hM4Di-mCherry-AAV10), strongly decreased the percentage time spent in SWS over a 2 hour post-CNO injection period as compared with vehicle injections (Supplementary Fig. 6). Hence, and in agreement with our previous findings, PZ GABAergic neurons also appear to be necessary for the initiation of normal SWS, even during times of high sleep drive.

CNO-induced SWS occurred at the expense of both wake (W) and rapid eye movement (REM) sleep, which were significantly decreased 3 and 9 hrs, respectively, following CNO administration (Fig. 3a,d). During the 3 hr post-CNO injection period, W bout duration was significantly decreased as compared with vehicle injections. Specifically, the preponderance of W amount occurred in 10s–10 min bouts following CNO administration, whereas most W amount occurred in bouts 10 min or longer following vehicle injections (Fig. 3e). During the remaining hours of the active (dark) period, and unlike that observed following the daytime CNO injections (Fig. 4a), W amount was significantly increased between 10PM and 7AM (Fig. 3a), suggesting that wake, like sleep, may also be under some level of homeostatic regulation, i.e., a wake rebound. With respect to REM sleep, its latency was significantly

increased (Fig. 3d and Supplementary Table 2) and REM sleep amount remained significant decreased over the remaining hours of the active period following CNO injection (Fig. 3d). During the subsequent light period, REM sleep amount returned to control levels, and no REM sleep rebound was seen, resulting in a net and significant decrease in REM sleep amount over the 24 hrs following CNO injection (46.6 ± 7.4 vs 72.8 ± 5.3 min after vehicle injection, $p = 0.0028$; $n = 13$). As SWS and wake homeostasis in general takes precedence over that for REM sleep, we also analyzed REM sleep on the second night following the 7PM CNO injections, but still found no evidence of REM recovery (Supplementary Table 2).

PZ directly inhibits BF-projecting PB neurons

In a previous study we showed that PZ sleep-active neurons project to the wake-promoting parabrachial nucleus (PB)¹³. Given that projections from glutamatergic PB neurons to the magnocellular basal forebrain (BFmc), but not the thalamus, are indispensable for maintaining cortical activation and wakefulness^{18, 19}, we hypothesized that GABAergic PZ neurons might promote SWS and SWA by inhibiting the wake-promoting PB-BFmc-cortex circuit. In other words, we predict that PZ GABAergic neurons monosynaptically project to and produce inhibitory postsynaptic events in PB neurons that specifically and monosynaptically innervate neurons of the BFmc. To test this hypothesis, we injected a cre-dependant vector containing channelrhodopsin-2 (DIO-ChR2(H134R)-mCherry-AAV; ChR2-mCherry) into the PZ and retrograde fluorescent microspheres were injected into the ipsilateral BFmc of *Vgat-ires-cre* mice (Fig. 5a). Histological assessment confirmed accurate bead placement in the BF (Fig. 5b-c) and mCherry-positive somas restricted to the GABAergic PZ (Fig. 5e-f). Photo-stimulation of PZ^{Vgat} cell bodies expressing ChR2-mCherry elicited robust photocurrents and trains of brief blue-light flashes entrained the firing of PZ^{Vgat} neurons up to 5 Hz (Supplementary Fig. 7). To determine whether activation of PZ axons evoked GABA release in the PB, we photostimulated PB slices containing ChR2-mCherry expressing axons that originated from PZ^{Vgat} neurons (Fig. 5d). The flashes of blue light evoked fast inhibitory postsynaptic currents (IPSCs) in PB neurons that were retrogradely labeled from the BFmc ($n = 7/18$ neurons). The light stimuli induced synaptic events of amplitude comparable to spontaneous IPSCs (Fig. 5h), indicating that the responses were in the physiological range. Moreover, based upon the rapid kinetics, both the spontaneous and photo-evoked responses occurred in the soma and proximal dendrites of the cell. The photo-evoked IPSCs were also completely abolished by bicuculline (20 μ M, Fig. 5g) indicating that these responses were mediated by the release of GABA and by the activation of GABA_A postsynaptic receptors. In BFmc-projecting PB neurons that exhibited synaptic responses (PZ^{Vgat}→PB) the probability of any given light pulse evoking a synchronous IPSC was $58.0 \pm 5.6\%$ ($n = 7$, Fig. 5i-j). Three stimuli were used to show that 1) the response was consistent across stimulation, and 2) no depression occurred following repeated stimulation, i.e., individual synaptic response had equivalent amplitudes. The photo-evoked IPSCs in PB neurons projecting to BFmc had an average onset delay of 6.2 ± 0.3 ms, a peak amplitude of 23.1 ± 3.2 pA, and a charge transfer of 1.02 ± 0.21 pC (single light pulses; $n = 7$). Photostimulation evoked IPSC's in PB neurons even in the presence of tetrodotoxin (TTX; $n = 4$; Fig. 5k) supporting a direct synaptic connectivity from PZ to PB (PZ^{Vgat}→PB→BFmc).

As neurons of the BFmc directly and heavily innervate the cerebral cortex (most regions and layers)²⁰ we sought to confirm, using a similar approach to the foregoing, that glutamatergic PB neurons monosynaptically project to and produce excitatory postsynaptic responses in cortically-projecting BF neurons. To do so we placed injections of ChR2-mCherry into the lateral PB and retrograde fluorescent microspheres into the ipsilateral prefrontal cortex (PFC) of *Vglut2-ires-cre* mice (n = 3; Fig. 5l). Histological assessment confirmed accurate bead placement in the PFC and mCherry-positive somas restricted to the glutamatergic lateral PB (Fig. 5m–n). To determine whether activation of PB axons evoked glutamate release in BFmc neurons that were retrogradely labeled from the PFC, we photostimulated slices containing ChR2-mCherry expressing axons that originated from PB^{Vglut2} neurons. The flashes of blue light evoked action potential firing and short latency excitatory postsynaptic currents (EPSCs) in cortically-projecting neurons of the BFmc (6/7 neurons; average onset delay: 5.9 ± 0.6 ms; n = 4) suggesting a direct synaptic connectivity from PB to BFmc (PB^{Vglut2}→BFmc→PFC). Responses to photostimulation in BFmc neurons were completely abolished by 6,7-dinitroquinoxaline-2,3-dione (DNQX; 30 μ M; Fig. 5o–q) indicating that these responses were mediated by the release of glutamate and by the activation of α -Amino-3-hydroxy-5-methyl-4-isoxazolepropionic acid (AMPA) postsynaptic receptors. In summary, GABAergic PZ neurons monosynaptically innervate and release synaptic GABA onto PB neurons that in turn project to and release synaptic glutamate onto cortically-projecting neurons of the BFmc. Hence the PZ^{Vgat}→PB^{Vglut2}→BFmc→PFC circuit represents a functional circuit substrate through which PZ GABA neurons can regulate cortical circuitry to potentially modulate behavioral state and EEG SWA (Supplementary Fig. 8).

Discussion

Batini's study in 1958 of the midpontine pretrigeminal preparation, which resulted in chronic insomnia (i.e., forebrain desynchrony), inspired the hypothesis that the caudal brainstem contained SWS-promoting/EEG synchronizing structures³. The location and existence of SWS-promoting/EEG synchronizing circuitry in the mammalian brainstem has however remained unresolved. In the present study we show, for the first time, that activation of a delimited node of GABAergic neurons located in the medullary PZ can potentially initiate SWS and cortical SWA in behaving animals. We further describe a functional, synaptic brainstem-forebrain-cortex pathway through which these neurons can modulate behavioral state and the cortical EEG.

PZ induces physiologic SWS and cortical SWA

There is every indication that the SWS and cortical SWA induced by activation of PZ GABAergic neurons in our experiments is physiologic. First, the power spectral distribution for CNO-induced SWS is identical to that of the "spontaneous" SWS observed following control injections. Second, as in normal SWS, we observed a gradual but persistent decrease in delta power over the course of the SWS episode²¹. Third, as expected of a "sleeping brain" c-Fos expression by cortical neurons was quiescent²². And, finally, a waking rebound was observed following the induction of SWS, indicating that CNO-induced SWS satisfied sleep need. A deeper inspection of the data further suggest that the CNO-induced SWS was,

in fact, a higher ‘quality’ SWS as compared with normal SWS. For example, delta power was higher and SWS bouts were longer as compared with normal SWS. This is reminiscent of the “deep” SWS observed following sleep deprivation^{23, 24}. In addition, CNO-induced SWS showed decreased power in the beta-gamma (20–60 Hz) band, which together with increased delta power is indicative of a high quality electrographic SWS²⁵. In sum, the increase in delta power at a time when delta is normally maximal (i.e., ZT12, which is the beginning of the dark period)^{9, 16}, the increase in SWS when sleep drive is normally maximal (i.e., ZT3), the short latency to SWS following CNO administration, and the length and consolidated nature of the CNO-induced SWS all strongly indicate that activation of PZ GABAergic neurons can rapidly and potently induces physiologic SWS and cortical SWA. Moreover, and consistent with a SWS-promoting function, acute inhibition of PZ GABAergic neurons – at a time of day approximating peak sleep drive – strongly decreased the percentage time spent in SWS.

It is also of interest that CNO-induced SWS at ZT12, which is a time that the mice are normally highly awake, resulted in an apparent “wake deprivation”. In other words, following CNO-induced SWS at ZT12, the mice showed a significantly greater amount of wake, indicating a wake “rebound”. In contrast, no wake rebound was observed following CNO-induced SWS at ZT3, which is a time that the mice are normally deeply asleep. Unlike wake, sleep deprivation is relatively easy to induce and study, and a homeostatic “rebound” of sleep following sleep deprivation is a widely accepted phenomenon in the sleep field. Our findings suggest that CNO-induced SWS at ZT12 may have produced a wake deprivation and a subsequent wake “rebound”, secondary to the induction of high quality SWS. That we only observed a wake “rebound” following CNO-induced SWS during the normal waking but not sleeping period, is further evidence that the wake “rebound” is directly linked to wake deprivation and not a non-specific response to CNO-induced SWS. Rather, we interpret this finding as evidence that wake, like sleep, may also be under some level of homeostatic regulation. This interpretation would be consistent with the vital biological role of wake, which is a behavioral state subserving a myriad of biological imperatives, including feeding and reproducing.

Interestingly, REM sleep was also inhibited during CNO-induced SWS and for a longer period than the apparent CNO-induced SWS effect. Why REM sleep was so strongly inhibited is unclear to us, but one explanation may be that the high SWS pressure followed by the high wake pressure prevented REM generation. This explanation, however, is not entirely consistent with the physiology observed following activation of PZ GABAergic neurons during the day-time. Specifically, following the CNO-induced SWS at ZT3, waking pressure did not appear to be higher, i.e., no apparent W “rebound” and normal amounts of SWS were observed far sooner than the 9h REM suppression observed. It is also the case that a previous study found that lesions of the rat PZ did not affect REM sleep quantity, whereas disruption of GABAergic transmission by PZ neurons in the mouse reduced REM sleep in proportion to SWS¹³. It therefore remains unclear if PZ GABAergic (or intermingled non-GABAergic PZ neurons) are involved in REM sleep control and thus we feel it is premature to assign a role for PZ in REM sleep control. It is also possible that PZ GABAergic neurons may project to and inhibit neurons that regulate the hippocampal and/or cortical EEG features of REM sleep, e.g., the precoeruleus region²⁶.

GABAergic PZ inhibits a major wake-promoting circuit

In this study we show that PZ GABAergic neurons project to and produce inhibitory postsynaptic events in presumptive wake-promoting PB neurons, which in turn project directly to the BFmc. This finding not only begins to establish a mechanism and substrate through which PZ GABAergic neurons can produce SWS and cortical SWA, but also links the PZ to circuitry previously established to play a key role in maintaining wakeful consciousness. For example, the PB→BF pathway is critically involved in EEG activation and wakefulness. Indeed, ablation of the PB or BF results in a coma-like state in rats, suggesting that an intact PB→BF pathway is an absolute requirement for desynchronization of the cortical EEG¹⁸. And while a PZ→PB projection was established in a previous study¹³ the neuronal phenotype and neurotransmitter used remained to be clarified. Here we show that PZ GABAergic neurons release synaptic GABA on BF-projecting PB neurons, suggesting not only a previously unrecognized source of potent inhibitory influence on the PB→BF pathway, but also a circuit substrate through which the PZ can modulate cortical activity. This contention is further supported by our ChR2-assisted mapping experiments demonstrating functional, synaptic connectivity between glutamatergic PB neurons and cortically-projecting BF neurons. In other words our optogenetic-based mapping experiments support a circuit model wherein activation of the PZ results in inhibition of the PB and hence the loss of excitatory drive to cortically-projecting BFmc neurons. The result is a decrease in the fast frequencies that are characteristic of cortical activation/desynchronization and wakefulness, which then directly or indirectly drives the appearance of slow waves and delta waves that are characteristic of cortical synchronization and SWS. Several aspects of this proposed circuit model remain to be tested and it may ultimately be the case that the PZ modulates cortical activity through other or additional ascending pathways/nodes. For now however it remains unclear if the PZ is interconnected with other sleep- and wake-promoting nodes beyond the wake-promoting PB. There are apparently projections to the PZ from hypocretin/orexin neurons in the lateral hypothalamus²⁷, however it is not clear whether these contact PZ sleep-promoting neurons. The VLPO apparently does not project to the PZ²⁸ and vice versa²⁹. Hence how the PZ may interact with other circuit elements of the “sleep switch” system remains an important area of future investigation.

It similarly remains unclear if the forebrain VLPO and the hindbrain PZ operate with any synergy to generate whole brain sleep. The SWS “phenotype” that develops following lesions of these structures are different, which suggest divergent roles for the VLPO and PZ in SWS regulation. Specifically, both VLPO and PZ lesions result in a ca. 50% decrease in daily SWS, yet the reduction in SWS after VLPO or PZ lesions derives from fundamentally different changes in SWS architecture. In the case of VLPO lesions, it is the duration of SWS episodes that is reduced³⁰ whereas in the case of PZ lesions it is the number of SWS episodes that is reduced¹³. To us these differences suggest that the VLPO may be more critically involved in SWS consolidation whereas the PZ is more critically involved in SWS initiation, although the extent to which the continued activity of PZ GABAergic neurons may contribute to the duration of the initiated SWS bout remains unknown. Regardless, future studies on animals with both VLPO and PZ lesions or dual activation/inactivation

studies will help clarify the extent to which the VLPO and PZ may work synergistically or, alternatively, function redundantly, in the production of SWS.

It is also worth mention that work reaching back many decades has suggested that the nucleus of the solitary tract (NTS) may comprise, at least in part, a SWS-promoting brainstem node^{5, 31}. While the NTS has the ability to modulate cortical activity and, importantly, our study does not preclude a SWS-promoting role for the NTS, there exist no data showing that NTS lesions produce insomnia or that they increase the amount of time spent awake³¹⁻³⁵, whereas PZ lesions do¹³. The PZ is, in fact, along the outflow tract from the NTS, and may receive its input, and so the PZ may, in addition to regulating the amount of SWS, serve as a link in an ascending pathway (vagal→NTS→PZ) that promotes sleep following, for example, a heavy meal, i.e., post-prandial somnolence.

In conclusion, in the present study we demonstrated that all polygraphic and neurobehavioral manifestation of SWS, including SWA, can be initiated in behaving animals by the selective activation of a delimited node of GABAergic medullary neurons. Our findings also suggest a synaptic brainstem-forebrain pathway through which these GABAergic PZ neurons can potently modulate behavioral state and cortical activity and may provide a structural basis for how brainstem inputs (Supplementary Fig. 8), including those that are activated by vagal nerve stimulators used to control epilepsy, may affect the forebrain EEG³⁶. These findings contribute to our understanding of how the brain regulates and organizes cycles of sleep-wake and may inform the development of drugs to better regulate states of sleep and wakefulness in patients with sleep or neurological disorders. This study moreover provides a new and potentially highly useful model system for the study of the SWS state and its regulation as well as for understanding the role of SWS in a continuum of physiologic and neurobiologic processes that SWS has been linked with, including energy metabolism, cognition, learning and cortical plasticity.

Supplementary Material

Refer to Web version on PubMed Central for supplementary material.

Acknowledgments

We are grateful to Quan Hue Ha, Minh Ha and Sarah Keating for superb technical assistance and Myriam Debruyne for helpful comments. We are also indebted to Drs. Bradford Lowell and Linh Vong for supplying us with the breeder pairs for developing our *Vgat-IRE5-cre* and *Vglut2-IRE5-cre* lines of mice. This work was supported by National Institutes of Health grants NS073613, NS061863, NS062727, NS061841, NS085477, DA024763, HL095491 and the G. Harold and Leila Y. Mathers Foundation.

References

1. Saper CB, Fuller PM, Pedersen NP, Lu J, Scammell TE. Sleep state switching. *Neuron*. 2010; 68:1023–42. [PubMed: 21172606]
2. Sherin JE, Shiromani PJ, McCarley RW, Saper CB. Activation of ventrolateral preoptic neurons during sleep. *Science*. 1996; 271:216–9. [PubMed: 8539624]
3. Batini C, Moruzzi G, Palestini M, Rossi GF, Zanchetti A. Persistent patterns of wakefulness in the pretrigeminal midpontine preparation. *Science*. 1958; 128:30–2. [PubMed: 13555923]
4. Affanni J, Marchiafava PL, Zernicki B. Higher nervous activity in cats with midpontine pretrigeminal transections. *Science*. 1962; 137:126–7. [PubMed: 14036582]

5. Bonvallet M, Bloch V. Bulbar Control of Cortical Arousal. *Science*. 1961; 133:1133–4. [PubMed: 17754758]
6. Dang–Vu TT, et al. Spontaneous neural activity during human slow wave sleep. *Proc Natl Acad Sci U S A*. 2008; 105:15160–5. [PubMed: 18815373]
7. Lu J, Greco MA, Shiromani P, Saper CB. Effect of lesions of the ventrolateral preoptic nucleus on NREM and REM sleep. *J Neurosci*. 2000; 20:3830–42. [PubMed: 10804223]
8. Vyazovskiy VV, Tobler I. The temporal structure of behaviour and sleep homeostasis. *PLoS One*. 2012; 7:e50677. [PubMed: 23227197]
9. Borbely, AA.; Achermann, P. Principles and Practice of Sleep Medicine. Kryger, MH.; Roth, T.; Dement, WC., editors. Elsevier Saunders; 2005. p. 405-417.
10. Marshall L, Helgadottir H, Molle M, Born J. Boosting slow oscillations during sleep potentiates memory. *Nature*. 2006; 444:610–3. [PubMed: 17086200]
11. Bushey D, Tononi G, Cirelli C. Sleep and synaptic homeostasis: structural evidence in *Drosophila*. *Science*. 2011; 332:1576–81. [PubMed: 21700878]
12. Massimini M, Huber R, Ferrarelli F, Hill S, Tononi G. The sleep slow oscillation as a traveling wave. *J Neurosci*. 2004; 24:6862–70. [PubMed: 15295020]
13. Anaclet C, et al. Identification and characterization of a sleep–active cell group in the rostral medullary brainstem. *J Neurosci*. 2012; 32:17970–6. [PubMed: 23238713]
14. Vong L, et al. Leptin action on GABAergic neurons prevents obesity and reduces inhibitory tone to POMC neurons. *Neuron*. 2011; 71:142–54. [PubMed: 21745644]
15. Tobler I, Borbely AA. Sleep EEG in the rat as a function of prior waking. *Electroencephalogr Clin Neurophysiol*. 1986; 64:74–6. [PubMed: 2424723]
16. Tobler, I. Principles and Practice of Sleep Medicine. Kryger, MH.; Roth, T.; Dement, WC., editors. Elsevier Saunders; 2005. p. 77-90.
17. Jones BE. Activity, modulation and role of basal forebrain cholinergic neurons innervating the cerebral cortex. *Prog Brain Res*. 2004; 145:157–69. [PubMed: 14650914]
18. Fuller P, Sherman D, Pedersen NP, Saper CB, Lu J. Reassessment of the structural basis of the ascending arousal system. *J Comp Neurol*. 2011; 519:933–56. [PubMed: 21280045]
19. Kaur S, et al. Glutamatergic signaling from the parabrachial nucleus plays a critical role in hypercapnic arousal. *J Neurosci*. 2013; 33:7627–40. [PubMed: 23637157]
20. Saper CB. Organization of cerebral cortical afferent systems in the rat. II. Magnocellular basal nucleus. *J Comp Neurol*. 1984; 222:313–42. [PubMed: 6699210]
21. Franken P, Tobler I, Borbely AA. Sleep homeostasis in the rat: simulation of the time course of EEG slow–wave activity. *Neurosci Lett*. 1991; 130:141–4. [PubMed: 1795873]
22. Lu J, et al. Role of endogenous sleep–wake and analgesic systems in anesthesia. *J Comp Neurol*. 2008; 508:648–62. [PubMed: 18383504]
23. Huber R, Deboer T, Tobler I. Effects of sleep deprivation on sleep and sleep EEG in three mouse strains: empirical data and simulations. *Brain Res*. 2000; 857:8–19. [PubMed: 10700548]
24. Franken P, Malafosse A, Tafti M. Genetic determinants of sleep regulation in inbred mice. *Sleep*. 1999; 22:155–69. [PubMed: 10201060]
25. Brown RE, Basheer R, McKenna JT, Strecker RE, McCarley RW. Control of sleep and wakefulness. *Physiol Rev*. 2012; 92:1087–187. [PubMed: 22811426]
26. Fuller PM, Saper CB, Lu J. The pontine REM switch: past and present. *J Physiol*. 2007; 584:735–41. [PubMed: 17884926]
27. Peyron C, et al. Neurons containing hypocretin (orexin) project to multiple neuronal systems. *J Neurosci*. 1998; 18:9996–10015. [PubMed: 9822755]
28. Sherin JE, Elmquist JK, Torrealba F, Saper CB. Innervation of histaminergic tuberomammillary neurons by GABAergic and galaninergic neurons in the ventrolateral preoptic nucleus of the rat. *J Neurosci*. 1998; 18:4705–21. [PubMed: 9614245]
29. Chou TC, et al. Afferents to the ventrolateral preoptic nucleus. *J Neurosci*. 2002; 22:977–90. [PubMed: 11826126]
30. Vetrivelan R, Fuller PM, Yokota S, Lu J, Saper CB. Metabolic effects of chronic sleep restriction in rats. *Sleep*. 2012; 35:1511–20. [PubMed: 23115400]

31. Magnes J, Moruzzi G, Pompeiano O. Synchronization of the EEG produced by low– frequency electrical stimulation of the region of the solitary tract. *Archives Italiennes de Biologie*. 1961; 99:33–41.
32. Reinoso–Barbero F, de Andres I. Effects of opioid microinjections in the nucleus of the solitary tract on the sleep–wakefulness cycle states in cats. *Anesthesiology*. 1995; 82:144–52. [PubMed: 7832296]
33. Laguzzi R, Reis DJ, Talman WT. Modulation of cardiovascular and electrocortical activity through serotonergic mechanisms in the nucleus tractus solitarius of the rat. *Brain Res*. 1984; 304:321–8. [PubMed: 6744045]
34. Puizillout JJ. Nucleus tractus solitarius, serotonin and regulation of vigilance. *Rev Electroencephalogr Neurophysiol Clin*. 1986; 16:95–106. [PubMed: 3532238]
35. Nosjean A, Arluison M, Laguzzi RF. Increase in paradoxical sleep after destruction of serotonergic innervation in the nucleus tractus solitarius of the rat. *Neuroscience*. 1987; 23:469–81. [PubMed: 3437976]
36. Schachter SC, Saper CB. Vagus nerve stimulation. *Epilepsia*. 1998; 39:677–86. [PubMed: 9670894]

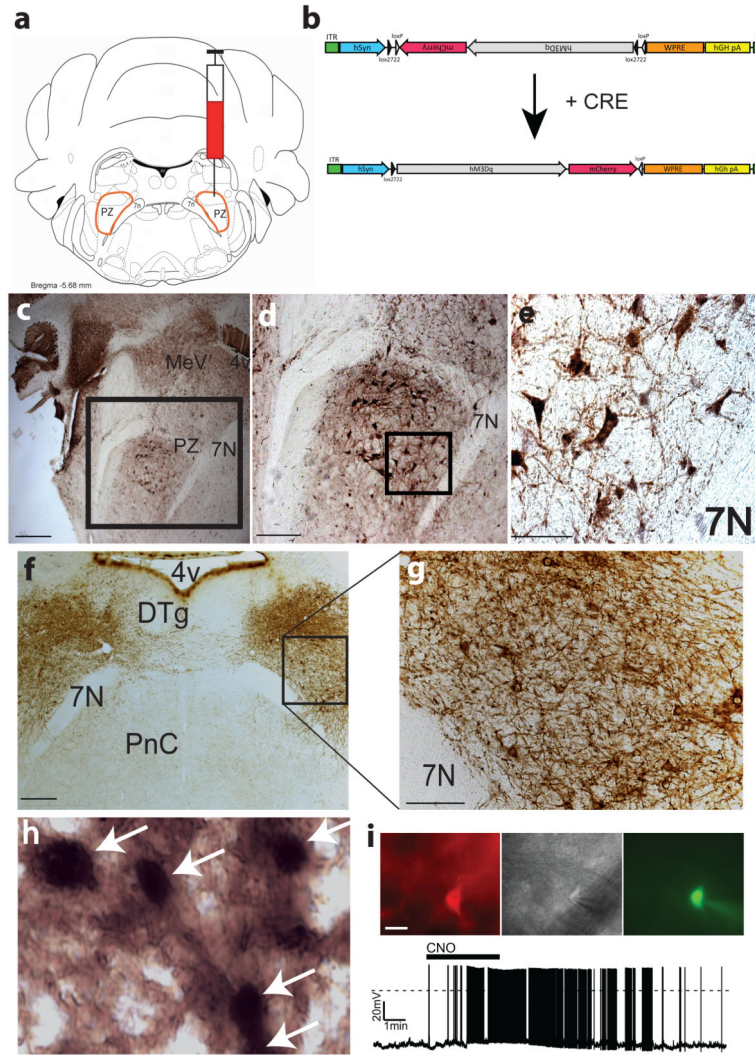


Figure 1. Cre-dependent expression of the hM3Dq receptor in PZ GABAergic neurons
(a) coronal section outline shows the injection target (delimited node of PZ GABAergic neurons) in *Vgat-IRES-cre* mice. **(b)** details of hSyn-DIO-hM3Dq-mCherry-AAV (hM3Dq-AAV) vector injected. **(c)** GFP immunolabeling in the brain of *Vgat-IRES-cre, lox-GFP* mice shows the location of GABAergic (VGAT+) PZ neurons (scale bar = 500 μ m); **(d)** higher power photomicrograph of GABAergic PZ neurons targeted for injection (scale bar = 250 μ m); **(e)** morphology of magnocellular PZ GABAergic neurons (scale bar = 65 μ m); **(f)** bilateral expression (brown immunoreactivity in neuropil) of the hM3Dq receptor in PZ GABAergic neurons following AAV-mediated transduction (scale bar = 300 μ m). **(g)** expression of hM3Dq receptors is evident on the cell surface and processes of GABAergic PZ soma (scale bar = 70 μ m). **(h)** high magnification image showing red-brown cytoplasmic and neuropil immunostaining with black nuclear c-Fos immunoreactivity indicates excitation of GABAergic hM3Dq+ PZ neurons by CNO (scale bar = 20 μ m). **(i)** CNO (500 nM bath applied) produced depolarization and firing in hM3Dq-expressing GABAergic PZ neurons in brain slices. 4v: fourth ventricle; 7n: facial nerve; Cre: cre-

recombinase; CNO: clozapine–N–oxide; DTg: dorsal tegmental nucleus; PnC: pontine reticular nucleus; PZ: parafacial zone.

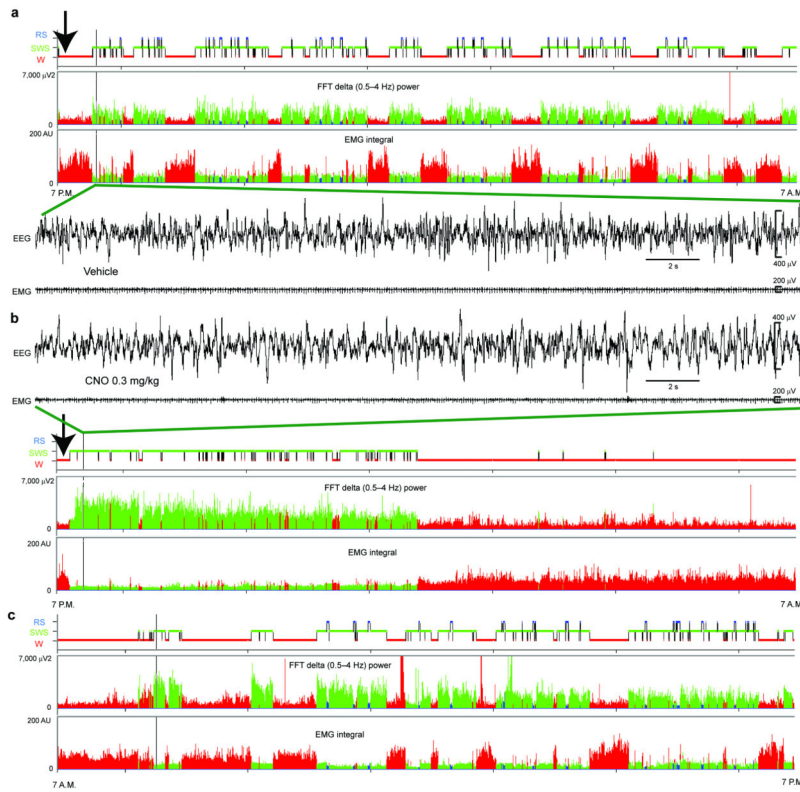


Figure 2. Administration of CNO induces all polygraphic manifestations of slow-wave-sleep (SWS) in mice expressing the hM3Dq receptor in GABAergic PZ neurons
 Example hypnogram, fast Fourier transform (FFT)-derived delta (0.5–4 Hz) power and EMG activity over 12 hrs following (a) vehicle (b) or CNO (0.3 mg/kg, IP; ZT12) administration in a mouse with bilateral hM3Dq receptor expression in PZ GABAergic neurons. Panel c shows the hypnogram, FFT-derived delta (0.5–4 Hz) power and EMG activity during 12 hr light period following panel b. The raw EEG and EMG traces following vehicle or CNO injection (arrow on the hypnogram) in 2a and b respectively provide unambiguous evidence of CNO-induced SWS/SWA in mice expressing hM3Dq in GABAergic PZ neurons. Note that, as compared to vehicle injection, CNO injection rapidly induced SWS, itself characterized by increased SWA density and amount. Color code: red = wakefulness (W), green = SWS and blue = REM sleep (RS). CNO: clozapine– N–oxide

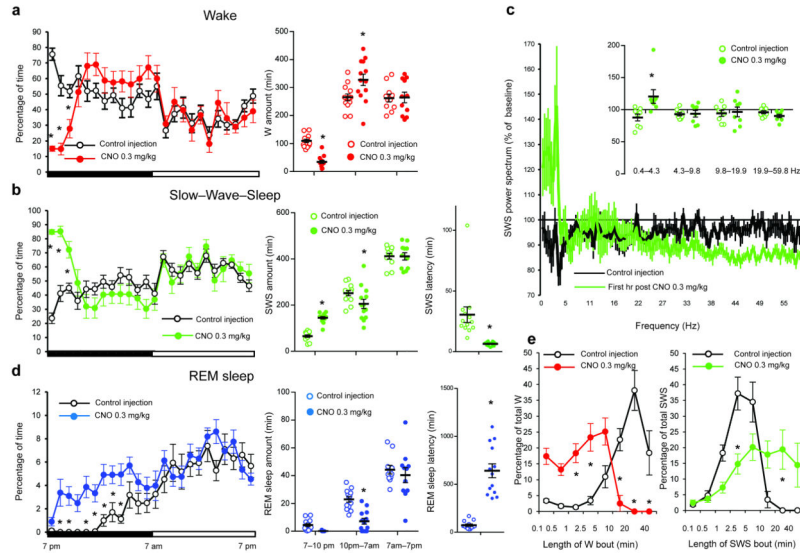


Figure 3. CNO administration promotes SWS at the expense of both wakefulness and REM sleep Panels **a**, **b** and **d** show the sleep–wake quantities following vehicle and CNO (0.3 mg/kg, IP; 7 P.M.; n = 13) injections in mice with bilateral expression of the hM3Dq receptor in PZ GABAergic neurons, including the average hourly sleep–wake amounts (% of time ± SEM); the total sleep–wake amounts (± SEM) during (1) the 3 hrs post–injection period (7PM–10PM), (2) the remainder (9 hours) of the dark/active period (10PM–7AM) and (3) the subsequent 12 hour light period (7AM–7PM); and the SWS and REM sleep latencies (± SEM). Panel **c** shows the SWS power spectrum changes (± SEM) over baseline during the 3 hr post–injection period for vehicle injection as compared with the first hour post–injection period for CNO (0.3 mg/kg, IP; ZT12; n = 8 mice) and the quantitative changes (± SEM) in power for the δ (0.4–4.3 Hz), θ (4.3– 9.8 Hz), α (9.8–19.9 Hz) and $\beta + \gamma$ (19.9–59.8 Hz) frequency bands (± SEM) following vehicle or CNO (0.3 mg/kg, IP; n = 8) administrations. In Panel **e** time–weighted frequency histograms show the proportion (± SEM) of W or SWS amounts in each bout length to the total amount of W or SWS in the 3 hours post–injection period following vehicle or CNO administration (0.3 mg/kg, IP; n = 13). CNO: clozapine–N–oxide two-way ANOVA followed by a *post hoc* Bonferroni test or paired T test * p < 0.05.

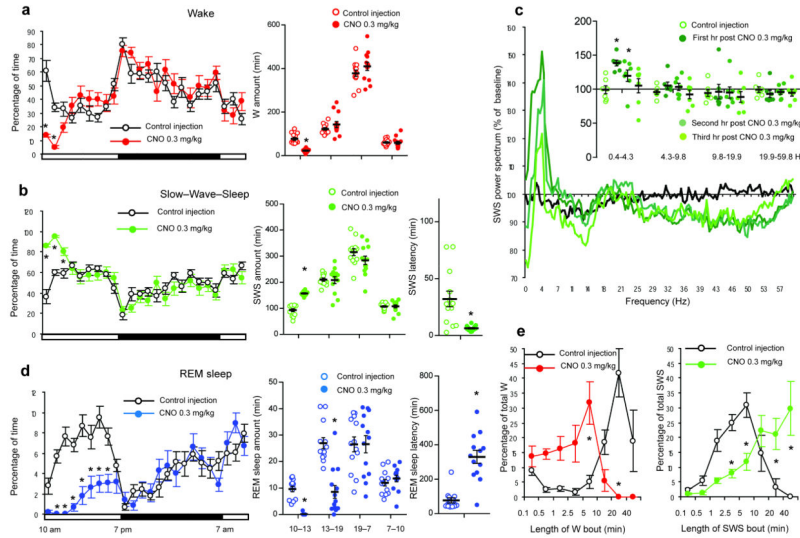


Figure 4. Activation of PZ GABAergic neurons increases slow-wave-sleep (SWS) during the subjective day

Panels **a**, **b** and **d** show sleep-wake quantities following vehicle and CNO (0.3 mg/kg, IP; 10 A.M.; n = 13) injections in mice with bilateral expression of the hm3Dq receptor in PZ GABAergic neurons, including the average hourly sleep-wake amounts (% of time ± SEM); the total sleep-wake amounts (± SEM) during (1) the 3 hrs post-injection period (10AM-1PM), (2) the remainder (6 hrs) of the light/sleep period (1PM-7PM), (3) the subsequent 12 hr dark period (7PM-7AM) and the next day first 3 hr of the light period (7AM-10AM); and the SWS and REM sleep latencies (± SEM). Panel **c** shows the SWS power spectrum changes over baseline during the 3 hr post-injection period for vehicle injection as compared with the first, second and third hour post-injection period for CNO (0.3 mg/kg; n = 7 mice) and the quantitative changes (± SEM) in power for the δ (0.4–4.3 Hz), θ (4.3–9.8 Hz), α (9.8–19.9 Hz) and $\beta + \gamma$ (19.9–59.8 Hz) frequency bands (± SEM) following vehicle or CNO (n = 7) administrations. In panel **e** time-weighted frequency histograms show the proportion (± SEM) of W or SWS amounts in each bout length to the total amount of W or SWS in the 3 hours post-injection period following vehicle or CNO administration (n = 13). CNO: clozapine-N-oxide; two-way ANOVA followed by a *post hoc* Bonferroni test or paired T test * p < 0.05.

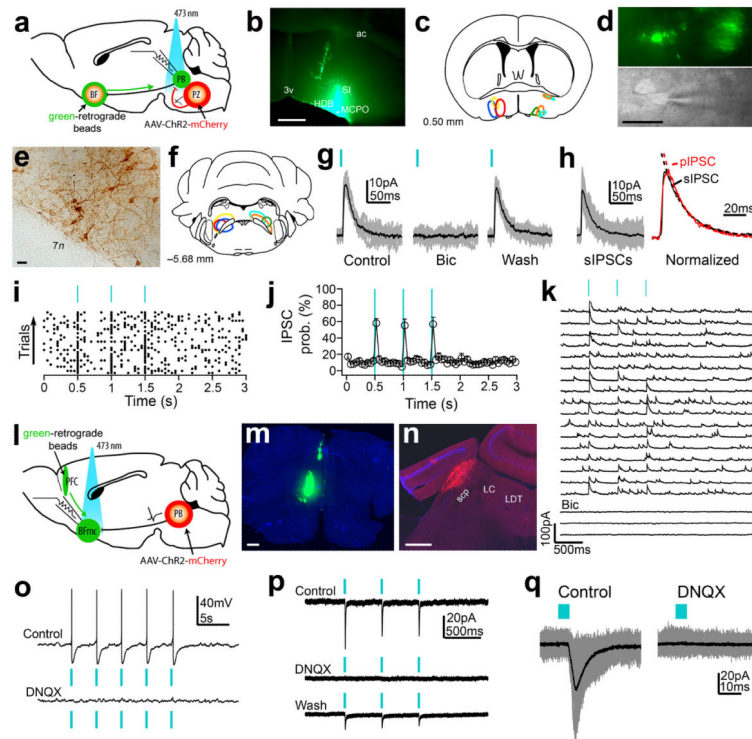


Figure 5. Channelrhodopsin-2-assisted circuit mapping to establish $PZ^{Vgat} \rightarrow PB \rightarrow BF$ and $PB^{Vglut2} \rightarrow BFmc \rightarrow PFC$ synaptic connectivity
(a–f) To map connectivity of 3rd-order downstream PZ^{Vgat} targets we injected green-retrograde beads into the BFmc (**b–c**) and DIO-ChR2-mCherry-AAV into the PZ of *Vgat-ires-cre* mice (**e–f**; mCherry immunoreactivity in brown) and we recorded retrogradely labeled PB neurons (**d**). **(g)** Photostimulation of PZ^{Vgat} terminals evoked GABAergic IPSCs in BFmc-projecting PB neurons **(h)** Photo-evoked IPSCs (pIPSCs) and spontaneous IPSCs (sIPSCs) had similar decay kinetics (single exponential fits SD: sIPSC = 0.013 and pIPSC = 0.023; τ : sIPSC = 19.02 ms and pIPSC = 18.70 ms). **(i–j)** Raster plot and average IPSC probability following photostimulation of $PZ^{Vgat} \rightarrow PB$ pathway (50 ms bin; $n = 5$; \pm S.E.M). **(k)** Photo-evoked GABAergic IPSCs recorded in TTX (1 μ M + 4-AP 1 mM), indicating monosynaptic connectivity. **(l–n)** To map $PB^{Vglut2} \rightarrow BFmc \rightarrow PFC$ connectivity we injected green-retrograde beads into the PFC and DIO-ChR2-mCherry-AAV into the PB of *Vglut2-ires-cre* mice (**m**, beads; **n**, mCherry native fluorescence). **(o–q)** Photostimulation of PB^{Vglut2} terminals produced glutamate release and spike firing in PFC-projecting BFmc neurons (**p–q**, $V_h = -60$ mV). Photostimulation: 5 ms pulses or 2 ms in **k**. Bicuculline-methiodide 20 mM and DNQX 30 μ M). Scale bars: 500 μ m in **b** and **m–n**; 30 μ m in **d–e**. Abbreviations: 3V, 3rd ventricle; 7n, facial nerve; ac, anterior commissure; BFmc, magnocellular basal forebrain; HDB, horizontal diagonal band of Broca; LC, locus coeruleus; LDT, lateraldorsal tegmental nucleus; MCPO, magnocellular preoptic nucleus; PB, parabrachial nucleus; PFC, prefrontal cortex; PZ: parafacial zone; scp: superior cerebral peduncle; SI: substantia innominate.